Temperature Dependent Measurement of GaN Impact Ionization Coefficients

L. Cao, Z. Zhu, G. Harden, H. Ye, J. Wang, A. Hoffman, and P. Fay

Department of Electrical Engineering, University of Notre Dame, 275 Fitzpatrick Hall, Notre Dame, IN 46556
(574) 631-5693; pfay@nd.edu

Keywords: GaN, breakdown, avalanche, impact ionization, temperature dependence

Abstract

Impact ionization imposes a fundamental limitation for devices in both RF power as well as power conversion and control applications. Especially for high-power devices, understanding of the temperature dependence of impact ionization is critical for device design. We report the measurement of impact ionization coefficients for both electrons and holes in GaN, including the effects of temperature. The extracted coefficients are found to be consistent with device breakdown measurements for a wide range of carrier concentration, device structures, and material growth techniques.

INTRODUCTION

GaN and other III-N materials are of obvious importance for terrestrial RF power applications, and are emerging as candidates for space RF as well as power conversion and control applications. As a result, developing an improved understanding of the fundamental physical limits of the technology is of increasing importance. A fundamental physical limit to the high-field handling performance of devices in GaN is impact ionization. We report measurement of the impact ionization properties of GaN, including the impact of elevated temperatures on impact ionization. These coefficients also enable the projection of the fundamental limitations of GaN-based devices; we find that our coefficients agree well with measured breakdown voltages for devices over a wide range of device design and material growth techniques.

DEVICE DESIGN AND CHARACTERIZATION

The experimental approach to measurement of impact ionization taken here is the use of the photomultiplication method, using the structures illustrated in Fig. 1. The structure in Fig. 1(a) includes a buried pseudomorphic InGaN layer to absorb the incident light, allowing pure hole injection into the drift layer when illuminated with 390 nm light. As illustrated in the band diagram in Fig. 1(a), the 390 nm wavelength illumination generates electron-hole pairs only in the InGaN layer, and the holes are subsequently injected into the drift layer. In contrast, the structure in Fig. 1(b) is used for electron injection. In this case, 193 nm wavelength light is used to generate electron-hole pairs near the surface of the p-GaN anode; the electrons diffuse to the drift layer resulting in pure electron injection into the drift layer. By measuring the reverse-biased current-voltage characteristics both in the dark and under illumination at different temperatures, the carrier multiplication can be determined and the resulting impact ionization coefficients can be extracted vs. temperature. For the devices reported here, the fabrication flow was similar to that reported in [1], including the use of an N(14) implant based edge termination. Device measurements were performed on-wafer in a shielded variable-temperature probe station.

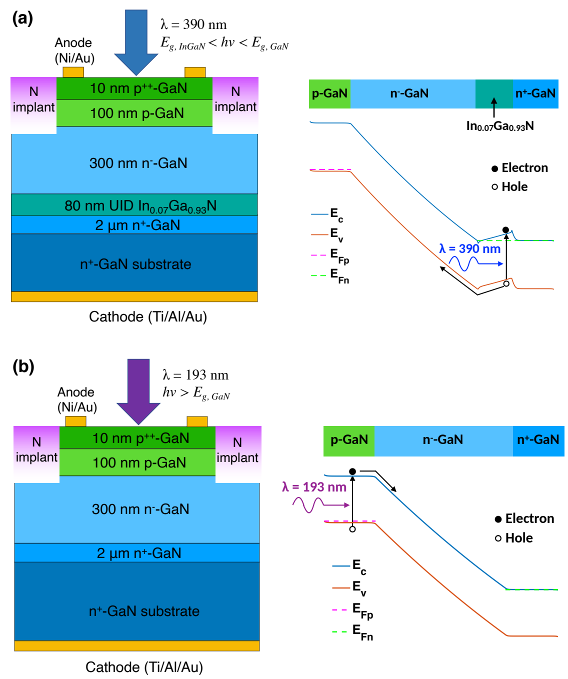

Fig. 1. Cross sections and illustrative band diagrams of device structures used for impact ionization coefficient measurement; (a) structure and band diagram for hole injection, (b) structure and band diagram for electron injection.

Figure 2 shows typical reverse-bias dark and illuminated measurements for both structures from which the extractions were performed. The devices show a positive temperature coefficient of breakdown, as expected for impact-ionization limited performance. The "shoulder" seen in the photocurrent response in Fig. 2(a) is caused by the polarization-induced barrier at the InGaN/GaN heterointerface, and influences only the low-field behavior of the device away from the onset of impact ionization.

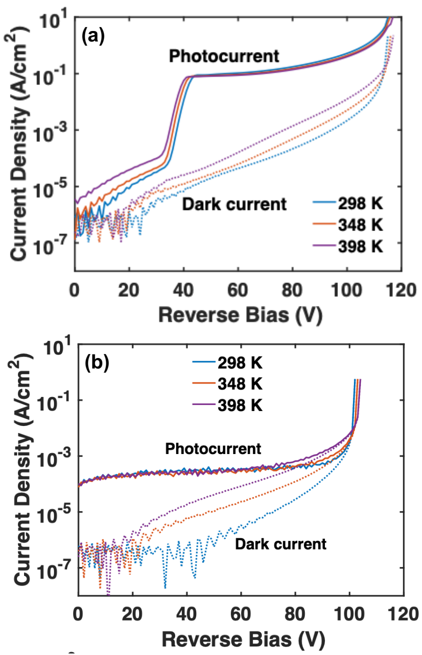

Fig. 2. Measured reverse-bias dark and illuminated I-V curves for: (a) hole injection using the structure in Fig. 1(a) with 390 nm illumination, and (b) electron injection using the structure in Fig. 1(b) with 193 nm illumination.

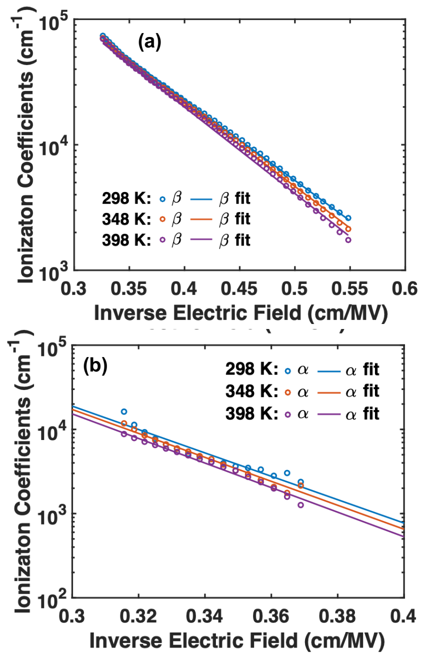

Fig. 3. Measured impact ionization coefficients for: (a) holes, β, and (b) electrons, α. Fits to the Okuto-Crowell model are also shown.

IMPACT IONIZATION COEFFICIENTS

From the measured characteristics in Fig. 2, the impact ionization characteristics can be extracted. For holes, the data in Fig. 2(a) can be used directly [2] under the assumptions that the field is uniform in the drift layer, that no electrons are injected, and that the impact ionization for holes is larger than that of electrons [3]. For the case of electrons, feedback between the electron and hole generation must be considered; we use the approach outlined in [4]; additional details on the extraction methodology can be found in [5].

The resulting temperature-dependent impact ionization coefficients for holes and electrons are shown in Fig. 3(a) and (b), respectively. Also shown in Fig. 3 are least-squares fits to the Okuto-Crowell model for temperature-dependent impact ionization [6]. In the Okuto-Crowell model, the impact ionization coefficients take the form of the Chynoweth model for impact ionization (equation (1) below) [7], but with temperature-dependent parameters *a(T)* and *b(T)* of the form shown in equations (2) and (3) [6]:

$$\alpha, \beta(E,T) = a(T)\exp\left(-\frac{b(T)}{E}\right) \tag{1}$$

$$a(T) = a_o(1 + c(T - T_o)) \tag{2}$$

$$b(T) = b_o(1 + d(T - T_o)) \tag{3}$$

Table 1 summarizes the coefficients obtained and the form of the model. Consistent with previous reports, the impact ionization coefficients for holes exceeds that of electrons (β/α = 5.3 at 3.3 MV/cm), in line with prior measurements and theoretical expectations [3, 8]. It is also noteworthy that the impact ionization coefficients are weak functions of temperature. This is promising for achieving device performance at high temperatures or self-heating conditions without significant off-state voltage derating.

As a check for consistency between measurement and the extracted parameters, the coefficients in Table 1 were used to simulate the hole and electron multiplication factors as a function of electric field for the device structures in Fig. 1; a comparison between the simulated and measured multiplication factors is provided in Fig. 4. As can be seen, excellent agreement is obtained over the full electric field range evaluated for both electrons and holes.

A critical issue for material parameter extractions like these is their predictive abilities for structures other than those used in the extraction process. Since the temperature coefficient of breakdown is controlled by impact ionization, this provides one means to assess the fidelity of the measured

Table 1. Impact Ionization Model and Extracted Parameters for GaN

Model: $\alpha, \beta(E,T) = a(T)\exp\left(-\frac{b(T)}{E}\right)$; $a(T) = a_o(1 + c(T - T_o))$; $b(T) = b_o(1 + d(T - T_o))$; E is electric field (V/cm), T is temperature (K).

Parameter	Electrons (α)	Holes (β)
a_o	$2.77\text{x}10^{8}$ cm^{-1}	$8.53\text{x}10^{6}$ cm^{-1}
b_o	$3.20\text{x}10^{7}$ V/cm	$1.48\text{x}10^{7}$ V/cm
c	$3.09\text{x}10^{-3}$ K^{-1}	$3.23\text{x}10^{-3}$ K^{-1}
d	$5.03\text{x}10^{-4}$ K^{-1}	$7.02\text{x}10^{-4}$ K^{-1}
T_0	298 K	298 K

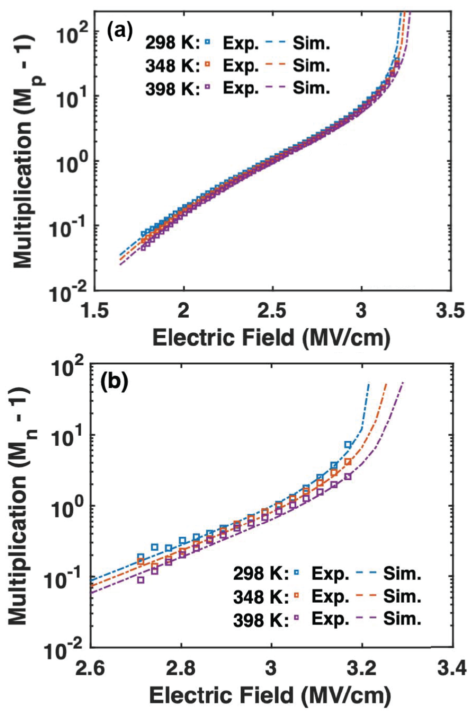

Fig. 4. Measured and simulated carrier multiplication factors for (a) holes and (b) electrons.

coefficients to experiment. The temperature dependence of breakdown in avalanche-limited devices is given by $BV(T) = BV_{298K}(1 + k\Delta T)$, where k is the temperature coefficient [9]. Figure 5 shows the temperature coefficient of breakdown extracted as a function of drift layer doping expected using the measured data reported here, as well as comparisons to measured avalanche-limited devices reported in the literature. As can be seen, good agreement between the measured temperature dependence of breakdown voltage and drift layer doping is observed.

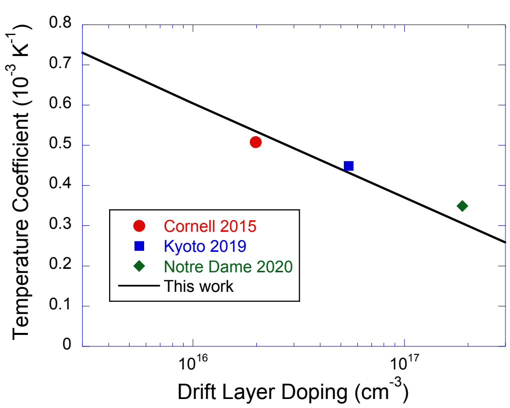

Fig. 5. Drift-layer doping density dependence of the temperature coefficient of breakdown from the reported coefficients (solid line) compared to literature reports for avalanche-limited devices [10-12].

To further assess the generality of the impact ionization coefficients reported here, Fig. 6 shows a comparison of the breakdown voltage vs. drift layer doping for a range of devices (FETs and diodes) reported in literature from a number of groups around the world [5, 13-32], as well as the avalanche-limited theoretical breakdown voltage based on the measured coefficients reported here. As can be seen, the model accurately bounds the experimental results from many groups, despite variations in material growth techniques, device structures, fabrication approaches, breakdown voltage, and carrier concentrations. This suggests the model and coefficients may be broadly applicable to GaN devices generally.

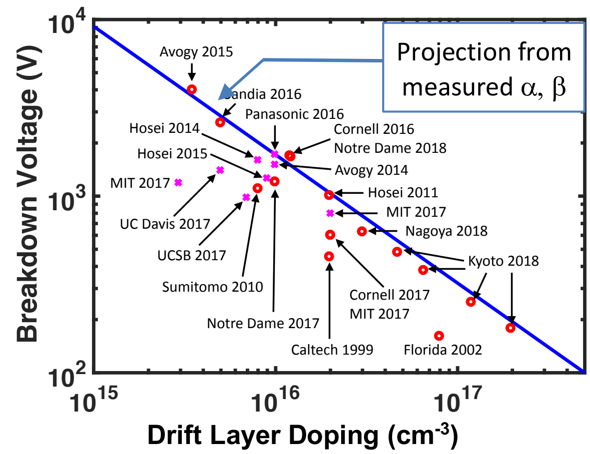

Fig. 6. Comparison of projected breakdown from impact ionization to measured breakdown in literature [5, 13-32].

Conclusions

The impact ionization coefficients for GaN as a function of temperature have been measured experimentally and compared to device performance. This will facilitate optimization of future RF and power device designs.

Acknowledgements

This work was supported in part by ONR, grant N00014-16-1-2850, Paul Maki program manager and ARPA-E, Isik Kizilyalli program manager.

References

[1] J. Wang et al., Appl. Phys. Lett., **113**, 0234502, 2018.
[2] H. Niwa et al., IEEE Trans. Electron Dev., **62**, 3326, 2015.
[3] L. Cao et al., Appl. Phys. Lett., **112**, 0262103, 2018.
[4] C. Lee et al., Phys. Rev., **134**, A761, 1964.
[5] L. Cao et al., IEEE Trans. Electron Dev., **68**, 2021.
[6] Y. Okuto and C. Crowell, Solid-State Electron., **18**, 161, 1975.
[7] A. G. Chynoweth, Phys. Rev., **109**, 1537, 1958.
[8] I. Oguzman et al., J. Appl. Phys., **81**, 7827, 1997.

[9] I. Kizilyalli et al., IEEE Trans. Electron Dev., **62**, 414, 2015.
[10] L. Cao, PhD dissertation, Univ. of Notre Dame, 2020.
[11] T. Maeda et al., IEEE Electron Dev. Lett., **40**, 941, 2019.
[12] Z. Hu et al., Appl. Phys. Lett., **107**, 243501, 2015.
[13] T. Oka et al., Appl. Phys. Exp., **8**, 054101, 2015.
[14] T. Maeda et al., Proc. IEDM, 30.1, 2018.
[15] Z. Bandic et al., Appl. Phys. Lett., **74** 1266, 1999.
[16] J. Johnson et al., IEEE Trans. Electron Dev., **49**, 32, 2002.
[17] Y. Saitoh et al., Appl. Phys. Exp., **3**, 081001, 2010.
[18] W. Li et al., IEEE Trans. Electron Dev., **64**, 1635, 2017.
[19] Y. Zhang et al., IEEE Electron Dev. Lett., **38**, 1097, 2017.
[20] K. Nomoto et al., Phys. Stat. Solidi A, **208**, 1535, 2011.
[21] Y. Zhang et al., Proc. IEDM, 10.2, 2016.
[22] K. Nomoto et al., IEEE Electron Dev. Lett., **37**, 161, 2016.
[23] O. Atkas and I. C. Kizilyalli, IEEE Electron Dev. Lett., **36**, 890, 2015.
[24] J. Dickerson et al., IEEE Trans. Electron Dev., **63**, 419, 2016.
[25] S. Usami et al., Appl. Phys. Lett., **112**, 182106, 2018.
[26] T. Oka et al., Appl. Phys. Exp., **7**, 021002, 2014.
[27] H. Nie et al., IEEE Electron Dev. Lett., **35**, 939, 2014.
[28] D. Shibata et al., Proc. IEDM, 10.1, 2016.
[29] M. Sun et al., IEEE Electron Dev. Lett., **38**, 509, 2017.
[30] C. Gupta et al., IEEE Electron Dev. Lett., **38**, 353, 2017.
[31] D. Ji et al., Proc. IEDM, 9.4, 2017.
[32] J. Wang et al., Appl. Phys. Lett., **113**, 023502, 2018.